

Spin-Polarized Electron Transport through Nanometer-Scale Al Grains

L. Y. Zhang, C. Y. Wang, Y. G. Wei, X. Y. Liu, and D. Davidovic
 Georgia Institute of Technology, Atlanta, GA 30332
 (Dated: February 8, 2020)

We investigate spin-polarized electron tunnelling through ensembles of nanometer scale Al grains embedded between two Co-reservoirs at 4.2K, and observe tunnelling-magnetoresistance (TMR) and the Hanle effect. The spin-coherence time (T_2^*), measured from the Hanle effect, is ns. Fast dephasing is attributed to electron spin-precession in the local fringing fields. Dephasing does not destroy TMR, in contrast to spin-relaxation. TMR is strongly asymmetric with bias voltage, which we explain by spin-relaxation. The voltage dependence of TMR is not simple and it is explained by a rapid decrease of the spin-relaxation time with bias voltage. This suggests that spin-relaxation in Al grains is concurrent with electronic relaxation, analogous to that in bulk.

Long spin relaxation times for polarized carriers are necessary for development of spintronic devices. In quantum dots, spin relaxation times are strongly enhanced compared to bulk, and the spin of an electron confined in a quantum dot is a candidate quantum bit [1, 2]. Unfortunately, the spin-coherence time T_2^* measured in a semiconducting quantum dot is only ns, despite the fact that the spin-relaxation time (T_1) is extremely long, up to a ms [4, 5].

Spin-injection and detection from ferromagnetic electron reservoirs is a well-known technique to measure spin relaxation time [6]. In this paper we study electron spin-injection in tunnelling junctions containing a large number of embedded Al-grains.

Tunnelling through an ensemble of grains has some advantages compared to tunnelling through a single grain. The current through an ensemble can be large even though the electron dwell times (τ_D) in individual grains are extremely long. In particular, to study spin-relaxation in grains, τ_D must be comparable to or longer than T_1 . Assuming T_1 ms, the current through individual grains must be comparable to $eT_1^{-1} \approx 10^{16}$ A, and this would be very difficult to measure. Tunnelling through an ensemble boosts the current in proportion with the number of grains.

Our tunnelling device is sketched in Fig. 1-A. The top and the bottom layers are 100Å thick Co films. The width/length is 1.5mm/15mm and 1mm/20mm for the bottom and the top layer, respectively. The sample cross-

section, sketched in Fig. 1-B, shows nanometer scale Al grains embedded in Al_2O_3 . The device is a recreation of a tunnelling device made by Zeller and Givier in the 1960s [7], which demonstrated Coulomb Blockade for the first time. The difference between our sample and the prior devices is that we have spin-polarized leads.

The device is fabricated in two evaporation steps. First, we thermally evaporate a Co film on a SiO_2 substrate, through a mask at 4×10^{-7} Torr pressure. Next, we deposit 2Å of Al at the same pressure. Then we introduce Oxygen at 3×10^{-5} Torr for 30sec, to oxidize the Al film. In the next step, we evaporate 5Å of Al at this pressure at 2Å/s, which creates the first Al_2O_3 film.

The sample is now exposed to air and the mask is replaced. Next, the sample is evacuated to base pressure and we deposit 15Å of Al, which creates isolated grains, as shown by the image in Fig. 1-C. Next, we deposit another layer of Al_2O_3 , using the same parameters as above. Finally, we deposit the top Co layer.

We assume that the grains have pancake shape. The average grain diameter is 6nm. Particle-in-a-box mean level spacing based on the diameter is 0.2meV. The number of grains is $N = 2.5 \times 10^6$. The sample resistances R are in the range $1k < R < 1M$ Ω. Note that there is a relatively wide distribution of grain diameters, as some grains have coalesced. Hence, the range of level spacings in the ensemble is large.

We also make tunnelling junctions as described above but without Al grains and find these devices to be insulating. In addition, we make control samples without Al grains and with the Al_2O_3 layers at half the thicknesses from those above. The control sample resistance is in the same range ($1k < R < 1M$ Ω).

We measured the surface roughness of a pure Al_2O_3 film by the atomic-force microscope and found that it was 5nm. The number of grains that are active in transport is N and it is not known, because of the nonuniform oxide thickness.

In this paper we present three devices. Fig. 2-A displays the IV-curve of sample 1 at 4.2K. The other two samples have similar IV-curves. The conductance is suppressed at zero bias voltage, as expected from Coulomb-

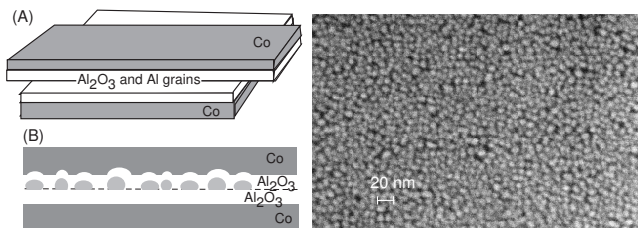


FIG. 1: A: Sketch of the tunnelling device geometry. B: Sketch of the tunnelling junction cross-section. C: Scanning electron micrograph of Al grains.

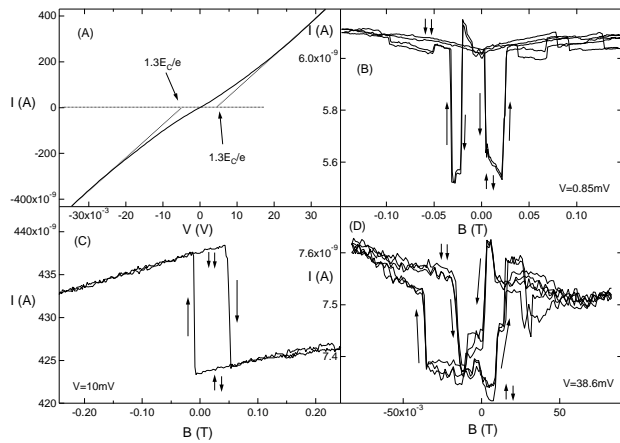


FIG. 2: A : IV -curves of sample 1 at 4.2K . B , C , and D : Current versus parallel applied magnetic field at 4.2K , in samples 1, 2, and 3, respectively.

Blockade on Al-grains, consistent with Ref. [7].

The average charging energy E_C is obtained by extrapolating the linear part of the IV-curve at high V to zero I and finding the offset voltage, as indicated. We averaged the Coulomb Staircase IV-curve [8] over the background charge, capacitance ratios, and over capacitance range ($C=4; 7C=4$), where C is the total capacitance of a grain. The corresponding offset was $1.3E_C=e$, where $E_C = e^2/2C$. E_C is 4.3meV in samples 1 and 2 and 6meV in sample 3.

Figs. 2-B, C, and D display current versus magnetic field in samples 1, 2, and 3 respectively, at constant bias voltage. All samples exhibit TMR, which demonstrates that the tunnelling current is spin-polarized. Samples 1 and 3 exhibit a spin-valve effect: at a large negative field, the magnetizations of the reservoirs are down. If the field increases, the magnetization of one Cobalt Co switches direction, and the tunnelling current drops discontinuously from $I_{\uparrow\uparrow}$ to $I_{\uparrow\downarrow}$. Finally, at a larger positive field the current jumps back up to $I_{\downarrow\downarrow}$.

Our Co -leads are multi-domain and we find that TMR fully saturates in the applied field of 1T. TMR is not reproducible among devices. In sample 2, for example, there is only one jump near zero field, followed by a broad TMR background that saturates only at B = 1T. We speculate that the TMR background and differences in TMR among samples arise from the strong magnetocrystalline anisotropy in Co and its competition with the shape anisotropy. Note that the top Co -layer is grown on a bumpy surface (Fig. 1-B).

Although we do not completely understand the TMR, we can still learn about spin-polarized tunnelling by focusing on the TMR-jumps near zero field. The jumps are reproducible, as seen in Fig. 2. The jump size estimates the spin-polarization of the current. For the Hanle effect, we select devices that exhibit the spin-valve effect.

The tunnelling magnetoresistance is calculated as

$$\text{TMR} = (I_{\uparrow\uparrow} - I_{\uparrow\downarrow})/I_{\uparrow\downarrow} \quad (1)$$

Figs. 3-A and B display differential conductance G with bias voltage in samples 1 and 2, respectively. G is measured by the lock-in technique. As the bias voltage is varied slowly at 3mV/hr, the magnetic field is swept between -0.25T and 0.25T at 0.01Hz. The differential conductance switches between $G_{\uparrow\uparrow}$ and $G_{\uparrow\downarrow}$ when the magnetizations switch alignment.

$G_{\uparrow\uparrow} - G_{\uparrow\downarrow}$ changes significantly when the bias voltage varies in a narrow interval around zero-bias voltage. In sample 2, the asymmetry in $G_{\uparrow\uparrow} - G_{\uparrow\downarrow}$ is dramatic: conductance is spin-unpolarized at negative bias and significantly spin-polarized at positive bias.

TMR also changes significantly around zero bias voltage, as shown in Fig. 3-C and D. Circles represent TMR from Eq. 1, and squares are obtained as $\text{TMR} = G_{\uparrow\uparrow}(V)dV - G_{\uparrow\downarrow}(V)dV$.

The spin-polarization of the current P is estimated by the Julliere model, [9] $\text{TMR} = 2P^2/(1 - P^2)$, where $P = (N_{\uparrow} - N_{\downarrow})/(N_{\uparrow} + N_{\downarrow})$ is the spin-polarization in the leads, and N_{\uparrow} and N_{\downarrow} are the spin-up and spin-down densities of states, respectively. At small positive bias voltage, TMR is 0.08 and 0.12 in samples 1 and 2, respectively. The corresponding values of P are 0.2 and 0.24, only 50% from the maximum possible P in Co . This demonstrates that spin-relaxation in the grains cannot be strong.

In high-quality magnetic tunnelling junctions, TMR is symmetric and weakly dependent on V. But in non-ideal magnetic tunnelling junctions, TMR can be asymmetric. [10, 11, 12, 13] The asymmetry has been explained by the two-step tunnelling via localized states. In our control samples, TMR is symmetric and weakly dependent on V, showing that the localized states responsible for asymmetric TMR are the electronic states in the grains.

We explain the asymmetry in TMR by the asymmetry between the average resistances between the grains and the two reservoirs. A symmetric resistances are easily introduced by sample fabrication. For example, exposure of the bottom Al_2O_3 layer to air increases the Al_2O_3 thickness by hydration.

The average dwell time is $\tau_D = \frac{R_D \hbar}{R_Q}$, where R_D is the average resistance between the grains and the drain reservoir, and $R_Q = 26k\Omega$. When the bias voltage changes sign, the drain reservoir changes, so τ_D also changes.

A symmetric TMR occurs when τ_1 is smaller than the longer dwell time. For example, in sample 2, figure 3-B suggests that τ_1 is much smaller than the dwell time at negative bias, and τ_1 is comparable to or longer than the dwell time at positive bias. The voltage interval around zero bias where the dwell times change is given by the Coulomb Blockade threshold $7k_B T = e$, in agreement with Fig. 3-A and B.

Next, we discuss the Hanle effect. We measure current versus magnetic field B_n applied perpendicular to

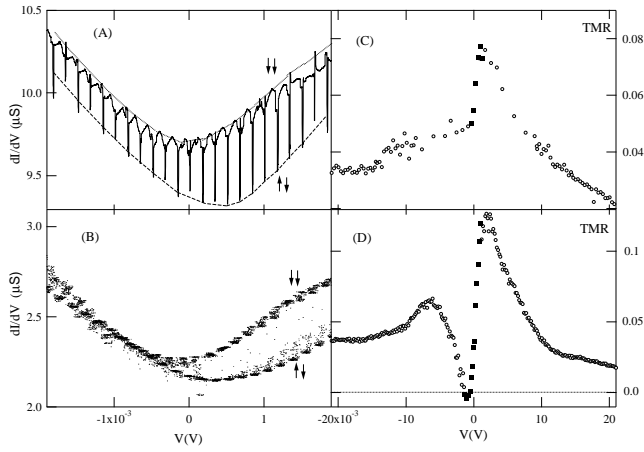


FIG. 3: A and B: Differential conductance versus bias voltage in samples 1 and 2, respectively. C and D: TMR versus bias voltage in samples 1 and 2, respectively.

the \ln . Fig. 4-A displays the resulting peak in current versus B_n , for sample 3 in the antiparallel configuration (in zero applied parallel field). The dependence is reversible when B_n is swept up and down, which shows that the curve does not arise from the hysteresis loop in the leads. The peak amplitude is $(I_{\uparrow} - I_{\downarrow}) = 2$.

The characteristic field B_C , defined as half-width of the peak, is 8 mT. We find that B_C is symmetric with bias voltage, which shows that B_C is independent of the dwell time. So, the processes that contribute to the Hanle effect half-width are different from the processes responsible for TMR asymmetry.

The Hanle effect in a quantum dot has recently been calculated by Braun et al. [14] The calculation shows that perpendicular field induces Larmor precession of the injected spin, which reduces spin polarization of the current. Current versus B_n exhibits a Lorentzian peak of amplitude $(I_{\uparrow} - I_{\downarrow}) = 2$ centered at $B_n = 0$. If a constant parallel magnetic field $B^?$ is present, then the peak width becomes $B^?$ in the limit of strong field ($B^? > \hbar = B_D; \hbar = T_1$) [14] and the Hanle effect half-width is symmetric with bias voltage.

Our observations can be explained by the these theoretical results, if we assume that there exist a local field acting on the grains in zero applied field. The local field varies among different grains and cannot be cancelled by the external field. Fig. 4-A then represents the distribution of the local field in the ensemble. The spin-coherence time is given by the Larmor period in the local field, $T_2^? = \hbar = B_C$ ns.

Among different samples, B_C is in the mT range and it varies among samples. Surface roughness, for example, can lead to a finite dipole field generated by Co. The local field of 8 mT is certainly possible, because the internal field in Co is 2T. The hyperfine field from the nuclei can also create an effective field of order mT. [3]

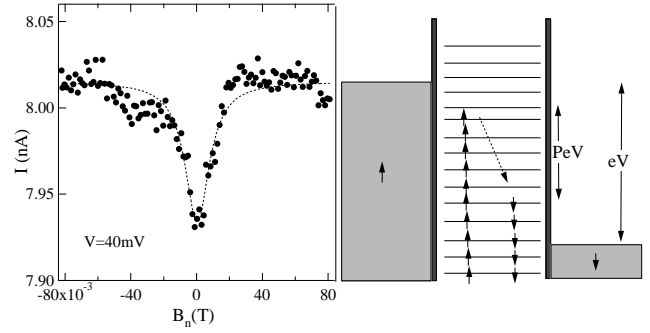


FIG. 4: A: Current versus perpendicular field in sample 3. B: Sketch of the grain electronic configuration at bias voltage V . The arrow indicates electron-phonon induced transition with spin flip.

In this explanation, TMR is finite despite the fact that $T_2^? = 0$. [14] By contrast, if $T_1 = 0$, then TMR will be suppressed to zero. TMR survives dephasing because of the conservation of spin-component along the local field direction. If the magnetizations switch from parallel to antiparallel state at finite V , then the spin-projection of the injected spin switch from zero to finite value and TMR is finite.

Now we discuss TMR versus V . At positive bias, where TMR is large, TMR is weakly dependent on V in interval $0.5 \text{ mV} < V < 3 \text{ mV}$. At larger voltage, TMR begins to decrease rapidly with V . At $V = 10 \text{ mV}$, the decrease in TMR with V slows down. At very large V , TMR is significantly reduced but not fully quenched to zero.

At negative bias voltage, where TMR is small, TMR is weakly dependent of V in interval $3 \text{ mV} < V < 0.5 \text{ mV}$. But, in sample 2, where TMR is fully quenched at $V = 0.5 \text{ mV}$, there is a maximum in TMR at around 8 mV. In sample 1, where TMR is not fully quenched at $V = 0.5 \text{ mV}$, there is a much weaker maximum around a similar voltage.

This dependence is complex, but it can be explained by a fast decrease in T_1 with V . This would be the case if spin-relaxation is caused by the electron-phonon energy relaxation in the presence of spin-orbit interaction, because electron-phonon relaxation time τ_{e-ph} decreases with V . This spin-relaxation mechanism is well known in bulk metals, where $T_1 = \tau_{e-ph} = (\text{Elliot-Yafet relation})$, and λ is the scattering ratio (10^{-4} in Al) [15]. The electron phonon relaxation time in metallic grains was calculated theoretically [16]

$$\frac{1}{\tau_{e-ph}(\lambda)} = \frac{2}{3} E_F^2 \frac{\lambda^3}{2 \hbar^4 v_s^5}; \quad (2)$$

where E_F is the Fermi energy (11.7 eV), λ is the ion-mass density (2.7 g/cm^3), v_s is the sound velocity (6420 m/s), λ is the excitation energy, and λ is the elastic scattering time. We are not aware of any theoretical calculation

that relates T_1 and τ_{e-ph} in a metallic grain.

At zero bias voltage, typical excitation energy at 4.2K is $3.5k_B T = 1.3m eV$. Eq. 2 gives the average transition time $\tau_{e-ph} (1.3m eV) = 60ns$ between the excited states at 4.2K. So, T_1 is longer than 60ns. If we assume that the Elliot-Yafet relation is valid in grains, we will obtain $T_1 = 60ns = m s$, which is comparable to T_1 in GaAs quantum dots. [5]

Note that we assume that the level spacing is $< k_B T$, so the transitions between the energy levels can be thermally driven. If the level-spacing is $> k_B T$, this relaxation mechanism is suppressed and T_1 is enhanced.

At finite bias voltage, we assume that the energy relaxation rate is larger than the escape rate, so that the distribution of electrons in the grain is in equilibrium (the basis of this assumption is as follows: TM R decreases with V suggests that $\tau_D > T_1$; since we expect $T_1 \tau_{e-ph}$, it follows that $\tau_D \tau_{e-ph}$, so electrons are in equilibrium).

In the antiparallel state, electron spins accumulate in the grains by transport, which creates a difference $P eV$ between the Fermi levels of spin up and spin down electrons, as shown in Fig. 4-B. However, if T_1 is shorter than the dwell time, then spin-up electrons in energy window $E_F - P eV = 2$ can undergo a transition into one of the unoccupied spin-down states at lower energies, as sketched by the arrow. TM R decreases with V because T_1 decreases with V , since electron-phonon transition time τ_{e-ph} decreases with V . This qualitatively explains TM R versus V at $V > 0$.

In this picture, TM R begins to decrease with V roughly when the spin-imbalance $P eV$ becomes comparable to $k_B T$, that is, when $V = k_B T / (P e) = 1.5m V$, in agreement with the data.

At $V = 10m V$, the decrease in TM R with V slows down, and TM R is not fully quenched at very large bias. In addition, TM R has a maximum at $10m V$. We suggest that these effects are caused by electron transport through small grains, in which $k_B T < \tau_{e-ph}$ (τ refers to small grains).

Near zero bias voltage ($V = k_B T = e$), only a very small fraction ($k_B T = E_C^S$) of small grains are conducting (because of Coulomb-Blochade), so TM R is dominated by electron transport through larger grains. Spin relaxation is fast in large grains, as discussed before, and it leads to asymmetric TM R. Spin-relaxation is suppressed in small grains, so small grains have large and symmetric TM R, but, their contribution to total TM R is reduced because of the Coulomb-Blochade.

At a large positive or negative bias, $V = \tau_{e-ph} = eP$, $5 \tau_{e-ph} = eP$, the fraction of conducting small grains increases to $eV = E_C^S = 5 \tau_{e-ph} = E_C^S$, which is of order 1. At this voltage, small grains still do not exhibit spin relaxation, because there is only one energy level in energy window $P eV$ in Fig. 4-B, so these grains have large and symmetric TM R at this bias voltage. Thus, TM R of the junction is en-

hanced at this voltage, which explains the slow down and the maximum at positive and negative voltages, respectively. With further increase in V , TM R of small grains begins to decrease, because the energy window $P eV$ becomes $> \tau_{e-ph}$.

In conclusion, we study spin-polarized current through ensembles of nm-scale Al grains. Tunneling magnetoresistance is asymmetric with current direction, which we attribute to the asymmetry in electron dwell times and spin-relaxation. The spin-coherence time is $T_2^* = ns$. Dephasing is attributed to spin-precession in the local fringing fields. The tunneling magnetoresistance has a complex voltage dependence, which is explained by a rapid decrease of the spin relaxation time T_1 with electron energy. Theoretical calculation of T_1 in metallic grains is desirable. Future research will try to increase T_2^* by the spin-echo technique.

This work was performed in part at the Georgia-Tech electron microscopy facility. This research is supported by the David and Lucile Packard Foundation grant 2000-13874 and Nanoscience/Nanoengineering Research Program at Georgia-Tech.

-
- [1] D. Loss and D. P. DiVincenzo, Phys. Rev. A 57, 120 (1998).
 - [2] G. Burkard, H. A. Engel, and D. Loss, Fortschr. Phys. 48, 965 (2000).
 - [3] A. C. Johnson, J. R. Petta, J. M. Taylor, A. Yacoby, M. D. Lukin, C. M. Marcus, M. P. Hanson, and A. C. Gossard, cond-mat/0503687 (????).
 - [4] T. Fujisawa, D. G. Austing, Y. Tokura, Y. Hirayama, and S. Tarucha, Nature 419, 278 (2002).
 - [5] J. M. Elzerman, R. Hanson, L. H. W. van Beveren, B. Witkamp, L. M. K. Vandersypen, and L. P. Kouwenhoven, Nature 430, 6998 (2004).
 - [6] M. Johnson and R. H. Silsbee, Phys. Rev. Lett. 55, 1790 (1985).
 - [7] H. R. Zeller and I. G. Iaver, Phys. Rev. 181, 789 (1969).
 - [8] D. V. Averin and K. K. Likharev, in Mesoscopic Phenomena in Solids, edited by B. L. Altshuler, P. L. Lee, and R. A. Webb (Elsevier and Amsterdam, 1991), p.169.
 - [9] M. Julliere, Phys. Lett. A 54, 225 (1975).
 - [10] J. Zhang and R. M. White, Jour. Appl. Phys. 83, 6512 (1998).
 - [11] E. Y. Tsybal, O. N. Mryasov, and P. R. LeClair, Jour. Phys. Cond. Mat. 15, R109 (2003).
 - [12] E. Y. Tsybal, A. Sokolov, I. F. Sabirianov, and B. Doudin, Phys. Rev. Lett. 90, 186602 (2003).
 - [13] J. R. Petta, S. K. Slater, and D. C. Ralph, Phys. Rev. Lett. 93, 136601 (2004).
 - [14] M. Braun, J. König, and J. Martinek, cond-mat/0411477 (????).
 - [15] F. J. Jedema, M. S. Nijboer, A. T. Filip, and B. J. van Wees, Phys. Rev. B 67, 085319 (2003).
 - [16] O. A. Gam, N. S. Wigngreen, B. L. Altshuler, D. C. Ralph, and M. Tinkham, Phys. Rev. Lett. 78, 1956 (1997).